JEE Journal of Ecological Engineering

Journal of Ecological Engineering 2023, 24(3), 90–98
https://doi.org/10.12911/22998993/157541
ISSN 2299–8993, License CC-BY 4.0

Received: 2022.11.19
Accepted: 2023.01.05
Published: 2023.01.15

Adsorption of Methyl Orange Dye by Modified Fly Ash-Based Geopolymer – Characterization, Performance, Kinetics and Isotherm Studies

Aprilina Purbasari[1*], Dessy Ariyanti[1], Evi Fitriani[1]

[1] Department of Chemical Engineering, Faculty of Engineering, Universitas Diponegoro, Semarang 50275, Indonesia

* Corresponding author's email: aprilina.purbasari@che.undip.ac.id

ABSTRACT

Geopolymer has been widely used as adsorbent for heavy metals and dyes. Modification on geopolymer surface with cationic surfactant can improve the anion exchange capacity of geopolymer. In this paper, fly ash-based geopolymer had been modified with cetyltrimethylammonium bromide (CTAB) which is cationic surfactant and applied as adsorbent of methyl orange (MO) anionic dye. Modified geopolymer had shown better performance as MO dye adsorbent compared to unmodified geopolymer. The adsorption of MO dye showed the best result at low pH and reached equilibrium after 90 minutes. On the basis of kinetics and isotherm studies, MO dye adsorption by modified geopolymer followed pseudo-second-order model and Langmuir model with maximum adsorption capacity of 19.231 $mg \cdot g^{-1}$.

Keywords: adsorption; methyl orange; modified fly ash-based geopolymer; CTAB surfactant.

INTRODUCTION

Geopolymer is inorganic polymer composed of tetrahedral silicate and aluminate units linked by sharing oxygen atoms. Geopolymer can be prepared from alumino-silicate materials, such as kaolin, fly ash, biomass ash, and slag (Davidovits, 2017; Samadhi et al., 2017). Geopolymer has amorphous to semi-crystalline three-dimensional structures and had been widely used as adsorbent. Many studies have reported that geopolymer can adsorb heavy metals and dyes. In geopolymer, tetrahedral aluminates have negative charge that can be balanced by exchangeable cations. Modification on geopolymer surface with cationic surfactant can improve the anion exchange capacity of geopolymer (Siyal et al., 2018; Selkala et al., 2020; Xu et al., 2022).

One of the most common dyes in textile industries is methyl orange (MO) dye. MO dye is also widely used as pH indicator in titration. MO dye is anionic azo dye that toxic and carcinogenic. Removal of MO dye in wastewater can be carried out by adsorption. Adsorption is a preferred method to remove MO dye because of its simplicity, high efficiency, and low cost in operation. Adsorbents used for MO dye removal include activated carbon, biochar, biosorbent, clays and minerals, polymers and resins, nanoparticles, and composites (Iwuozor et al., 2021; Wu et al., 2021).

In this paper, fly ash-based geopolymer was modified with cetyltrimethylammonium bromide (CTAB) which is cationic surfactant and applied as MO dye adsorbent. The characterization of modified fly ash-based geopolymer was studied in addition to its performance as MO dye adsorbent with variable of pH, time, and initial concentration. Furthermore, the studies of adsorption kinetics model and adsorption isotherm model had also been conducted.

MATERIALS AND METHODS

The fly ash waste used in this research was obtained from a power plant in East Java, Indonesia, and contained main oxides: SiO_2 (32.4%), Al_2O_3

(16.4%), Fe_2O_3 (23.8%), CaO (19.3%), MgO (2.6%), and K_2O (1.8%). Other materials used in this research were commercial NaOH flakes (98%), Na-silicate solution (35%), H_2O_2 solution (30%), HNO_3 solution (65%), cetyltrimethylammonium bromide (CTAB), methyl orange (MO), and distilled water.

Fly ash was first sieved with 100 mesh standard sieve and then mixed with alkaline activator with mass ratio of 2.5:1 in a planetary mixer at low speed for 10 minutes. Alkaline activator consisted of 10 N NaOH solution and Na-silicate solution with mass ratio of 1:1. H_2O_2 was added to the mixture in the amount of as much as 1 %-mass and stirred for 2 minutes. Geopolymer paste was cast in 5 × 5 × 5 cm molds. After 24 hours, the geopolymer was removed from molds and heated in oven at 60 °C for 6 hours. The geopolymer was then crushed and used as dye adsorbent. For modified geopolymer, crushed geopolymer was mixed with 0.01 M CTAB surfactant solution for 2 hours. Modified geopolymer was then sieved, washed with distilled water, and dried in oven at 100 °C for 1 hour.

Characterization of fly ash, geopolymer, and modified geopolymer consisted of Fourier transform infrared (FTIR) analysis using PerkinElmer Spectrum IR spectrometer and scanning electron microscope (SEM) analysis using JEOL JSM 6510 LA instrument.

Adsorptions of MO dye by geopolymer and modified geopolymer with dose of 2 g.L^{-1} were performed in batch process at various pH (2, 4, 7, 10, 12), time (15, 30, 45, 60, 75, 90, 105, 120 minutes), and initial concentration of MO dye solution (10, 20, 30, 40, 50, 60, 70, 80, 90, 100 mg·L^{-1}) at room temperature and stirring rate of 200 rpm. The concentration of MO dye solution was analyzed using Thermo Scientific Genesys 10S UV-Vis spectrophotometer.

Efficiency of MO dye removal (%) can be calculated with the equation:

$$MO\ dye\ removal\ efficiency\ (\%) = \\ = \frac{C_0 - C_e}{C_0} \times 100 \quad (1)$$

where: C_0 – initial concentration of MO dye solution (mg·L^{-1});
C_e – concentration of MO dye solution at equilibrium (mg·L^{-1}).

Adsorption kinetics studies were carried out using pseudo-first-order, pseudo-second-order, and Elovich, models which can be expressed by following equations:

$$\ln(q_e - q_t) = lnq_e - k_1 t \quad (2)$$

$$\frac{t}{q_t} = \frac{1}{k_2 q_e^2} + \frac{t}{q_e} \quad (3)$$

$$q_t = \frac{1}{\beta} ln\alpha\beta + \frac{1}{\beta} lnt \quad (4)$$

At those equations, q_t denotes the adsorption capacity at time t (mg·g^{-1}) and q_e denotes the adsorption capacity at equilibrium (mg·g^{-1}). Adsorption capacity can be calculated using this equation:

$$q = \frac{(C_0 - C_e)V}{W} \quad (5)$$

where: V – volume of MO dye solution (L);
W – mass of adsorbent (g) (Benjelloun et al., 2021; Khan et al., 2022; Nizam et al., 2021).

Furthermore, adsorption isotherm studies were conducted using Langmuir, Freundlich, and Temkin, models which can be stated by these equations:

$$q_e = \frac{q_m K_L C_e}{1 + K_L C_e} \quad (6)$$

$$q_e = K_F C_e^{\frac{1}{n}} \quad (7)$$

$$q_e = \frac{RT}{b} \ln(K_T C_e) \quad (8)$$

The value of q_m denotes the maximum adsorption capacity (mg·g^{-1}) (Al-Ghouti and Al-Absi, 2020; Mobarak et al., 2018; Wang and Guo, 2020).

RESULTS AND DISCUSSION

Characterization of fly ash, geopolymer, and modified geopolymer

The FTIR spectra of fly ash, geopolymer, and modified geopolymer at wavenumber of 4000–500 cm^{-1} are shown in Figure 1. Fly ash and the geopolymer from fly ash showed almost the same spectra. Meanwhile, there were new peaks at 2925 cm^{-1}, 2855 cm^{-1}, and 1452 cm^{-1} on the modified geopolymer from fly ash. Peaks at 2925 cm^{-1}

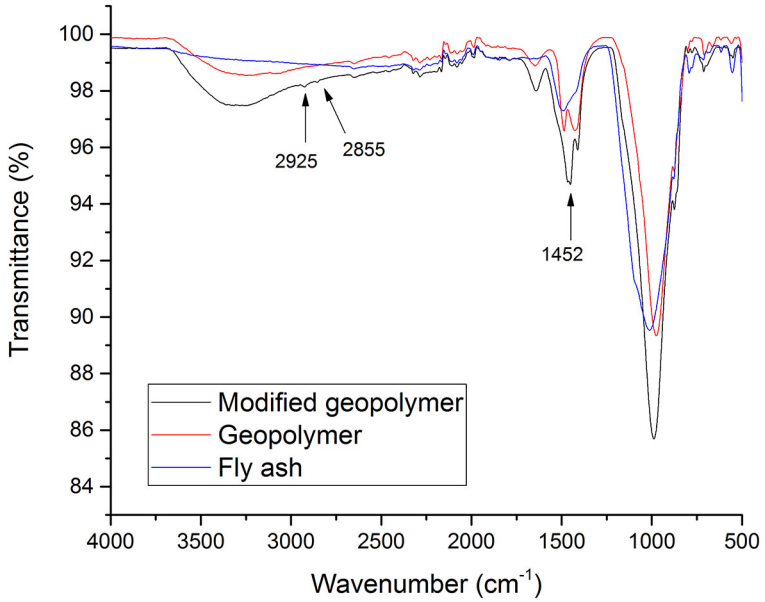

Figure 1. FTIR spectra of fly ash, geopolymer, and modified geopolymer

and 2855 cm^{-1} corresponded to asymmetric and symmetric stretching vibrations of $-CH_3$ and $-CH_2$. Peak at 1452 cm^{-1} attributed to bending vibration of the methylene groups. These results denoted the presence of CTAB surfactant on the surface of the modified geopolymer (Huang et al., 2017; Mobarak et al., 2018; Selvi et al., 2018; Yu et al., 2020).

The microstructure of fly ash, geopolymer, and modified geopolymer can be observed from

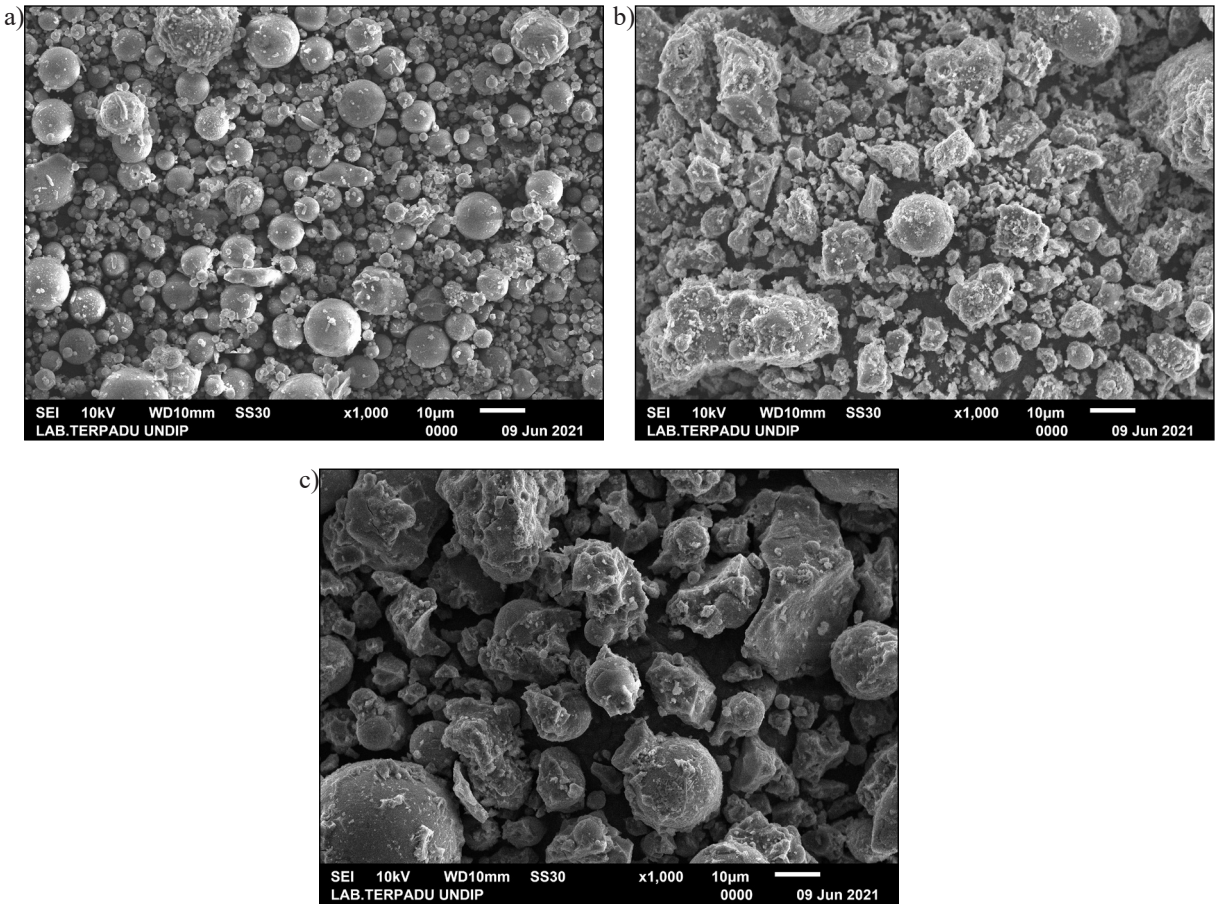

Figure 2. Scanning electron micrographs of fly ash (a), geopolymer (b), and modified geopolymer (c)

SEM images with magnification of 1000x as shown in Figure 2. Fly ash consisted of spherical particles of various sizes. On the geopolymer from fly ash, continuous phase resulting from geopolimerization process appeared as obtained in previous studies (Purbasari et al., 2018; El Alouani et al., 2019). As for modified geopolymer, its surface looked smoother due to CTAB surfactant coatings.

Performance of geopolymer and modified geopolymer as MO dye adsorbent

Performance of geopolymer and modified geopolymer from fly ash as MO dye adsorbent was studied by varying pH, time, and initial concentration. The effect of pH on MO dye removal efficiency by geopolymer and modified geopolymer is shown in Figure 3. In this adsorption process, 100 mL MO dye solution with concentration of 50 mg·L^{-1} was adsorbed by 0.2 g adsorbent for 2 hours. The removal efficiency of MO dyes tended to decrease up to pH of 12 using both geopolymer and modified geopolymer adsorbents. The highest removal efficiency of MO dye was obtained at pH of 2. In low pH or acidic solution, adsorbent surface becomes positively charged from hydrogen ions (H^+) so that MO anionic dye can be adsorbed easily on adsorbent surface (Fumba et al., 2014; Robati et al., 2016).

Figure 4 shows the effect of time on MO dye removal efficiency by geopolymer and modified geopolymer. Adsorption process was carried out using 100 mL MO dye solution with

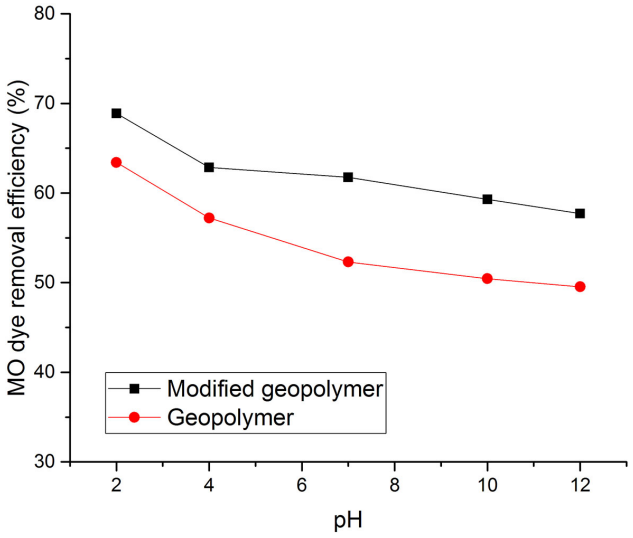

Figure 3. The effect of pH on MO dye removal efficiency

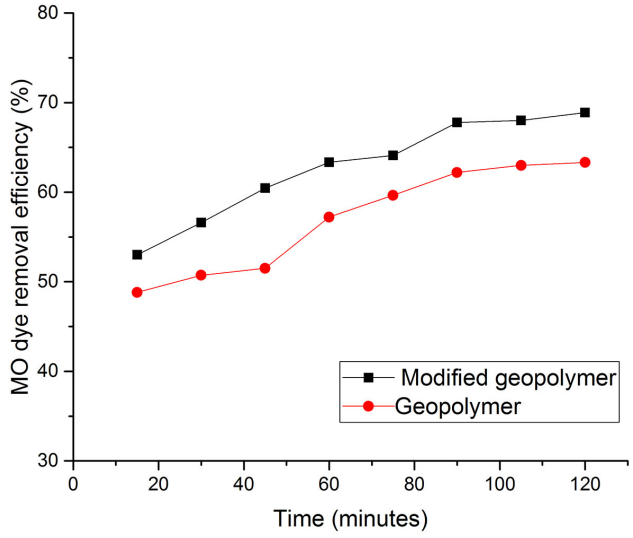

Figure 4. The effect of time on MO dye removal efficiency

concentration of 50 mg·L^{-1}, adsorbent dose of 0.2 g, and pH of 2. The MO dye removal efficiency increased along with time and was relatively constant after 90 minutes using both geopolymer and modified geopolymer adsorbents. At initial stage of adsorption process, the rate of MO dye removal was high, because there were still many available active sites on adsorbent surface. After equilibrium stage was reached, there were fewer available active sites on adsorbent surface so that the rate of MO dye removal became slower (Robati et al., 2016; Fernandes et al., 2020).

The effect of initial concentration on MO dye removal efficiency by geopolymer and modified geopolymer was studied using 100 mL MO dye solution with dose of adsorbent of 0.2 g and pH of 2 for 2 hours. The result in Figure 5 showed that the increase of the initial MO dye concentration can decrease the removal efficiency for both geopolymer and modified geopolymer adsorbents. The number of active sites on adsorbent surface can support the adsorption process at low initial concentration, but the active sites are no longer sufficient to support the adsorption process at high initial concentration (Robati et al., 2016; Fernandes et al., 2020).

The results of MO dye adsorption using geopolymer and modified geopolymer with variations in pH, time, and initial concentration showed that removal efficiencies of MO dye by modified

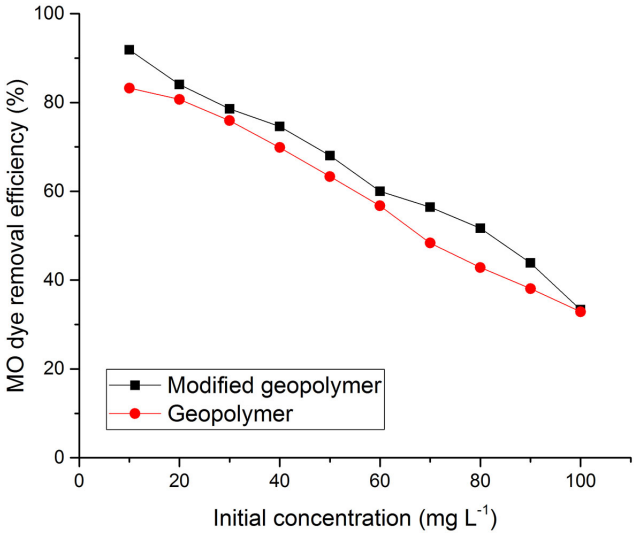

Figure 5. The effect of initial concentration on MO dye removal efficiency

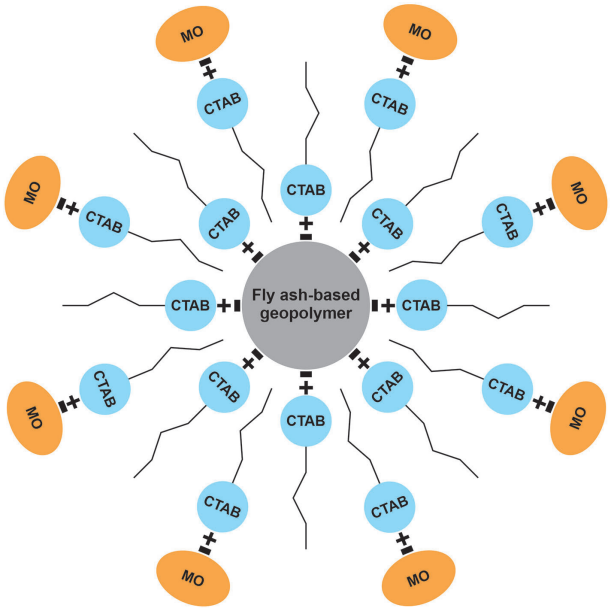

Figure 6. Illustration of MO anionic dye adsorption by modified fly ash-based geopolymer

geopolymer were higher than that by geopolymer. The presence of CTAB cationic surfactant on the negatively charged geopolymer surface can be illustrated as presented in Figure 6. This modification can increase the adsorption capacity of geopolymer on MO anionic dye (Mahmoodi et al., 2014; Selkala et al., 2020).

Kinetics studies of MO dye adsorption by modified fly ash-based geopolymer

Kinetics studies of MO dye adsorption by modified fly ash-based geopolymer were carried out using pseudo-first-order, pseudo-second-order, and Elovich models. In pseudo-first-order kinetics model, adsorption process is assumed to be controlled by diffusion. Meanwhile, in pseudo-second-order kinetics model, adsorption process is assumed to be controlled by chemical adsorption. As for Elovich kinetics model, adsorption process is assumed to be controlled by chemical adsorption on heterogeneous surface (Benjelloun et al., 2021; Khan et al., 2022; Nizam et al., 2021). Kinetics parameters for each kinetics model can be obtained by plotting linear equation (2) for pseudo-first-order model ($ln(q_e - q_t)$ versus t), plotting linear equation (3) for pseudo-second-order model (t/q_t versus t), and plotting linear equation (4) for Elovich

Table 1. Kinetics parameters and squared-correlation coefficients for MO dye adsorption by modified fly ash-based geopolymer

Pseudo-first-order model			Pseudo-second-order model			Elovich model		
q_e (mg·g^{-1})	k_1 (min^{-1})	R^2	q_e (mg·g^{-1})	k_2 (g·mg^{-1}·min^{-1})	R^2	α (mg·g^{-1}·min^{-1})	B (mg·g^{-1})	R^2
8.482	0.033	0.921	18.518	0.006	0.998	84.909	0.495	0.979

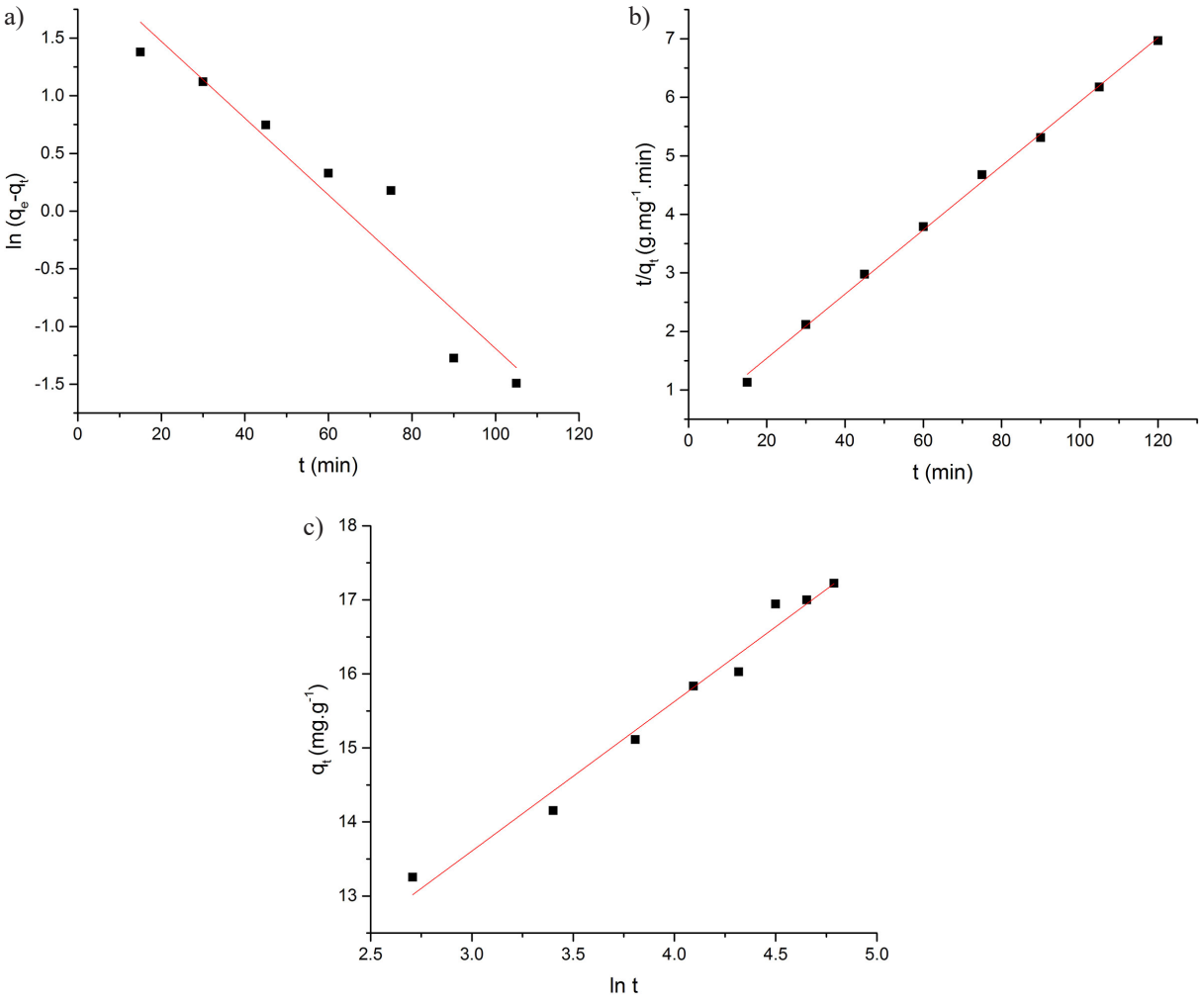

Figure 7. Linear plots of pseudo-first-order (a), pseudo-second-order (b), and Elovich (c) kinetics models for MO dye adsorption by modified fly ash-based geopolymer

model (q_t versus $ln\ t$) as shown in Figure 7. Table 1 represents kinetics parameters and squared-correlation coefficients (R^2) for each kinetics model. Pseudo-second-order kinetics model had the highest R^2 value so that MO dye adsorption by modified fly ash-based geopolymer followed pseudo-second-order kinetics model. Thus, the adsorption process was controlled by chemical adsorption.

Isotherm studies of MO dye adsorption by fly ash-based geopolymer

Isotherm studies of MO dye adsorption by modified fly ash-based geopolymer were conducted using Langmuir, Freundlich, and Temkin models. Langmuir isotherm model considers monolayer adsorption due to homogeneous adsorbent surface, while Freundlich isotherm model considers multilayer adsorption because of heterogeneous adsorbent surface having different adsorption abilities. Moreover, Temkin isotherm model considers uniform distribution of binding energies on adsorbent surface (Al-Ghouti and Al-Absi, 2020; Mobarak et al., 2018; Wang and Guo, 2020). By plotting linear equation (6-8), namely C_e/q_e versus C_e, $log\ q_e$ versus $log\ C_e$, and q_e versus $ln\ C_e$ as shown in Figure 8, isotherm parameters for each model can be obtained. Isotherm parameters and

Table 2. Isotherm parameters and squared-correlation coefficients for MO dye adsorption by modified fly ash-based geopolymer

Langmuir Model			Freundlich Model			Temkin Model		
q_m (mg·g^{-1})	K_L (L·mg^{-1})	R^2	1/n	K_F (mg·g^{-1}·(L·mg^{-1})$^{1/n}$)	R^2	K_T (L·g^{-1})	B (J·mol^{-1})	R^2
19.231	0.525	0.974	0.327	5.888	0.889	4.633	684.844	0.884

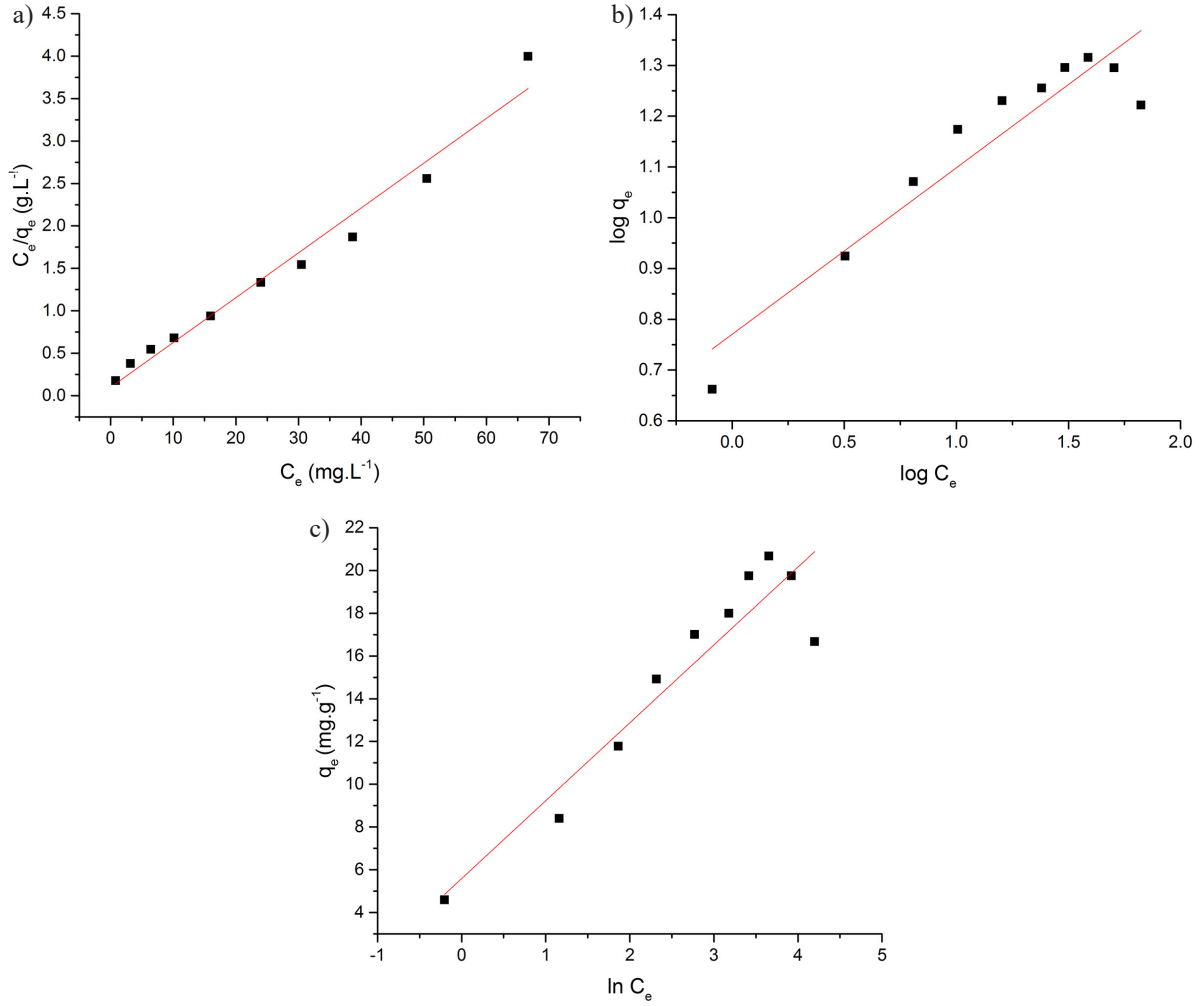

Figure 8. Linear plots of Langmuir (a), Freundlich (b), and Temkin isotherm models for MO dye adsorption by modified fly ash-based geopolymer

Table 3. Maximum adsorption capacity of MO dye by various adsorbents

Adsorbent	Maximum adsorption capacity (mg·g^{-1})	References
Activated clay	16.78	Ma et al. (2013)
Geopolymer from metakaolin	3.393	Fumba et al. (2014)
Graphene oxide	16.83	Robati et al. (2016)
Fly ash	3.9	Potgieter et al. (2021)
Chrysotile nanotubes	31.46	Wu et al. (2021)
Anion exchange membrane	18	Khan et al. (2022)
Modified fly ash-based geopolymer	19.231	This study

squared-correlation coefficients (R^2) for each isotherm model are presented in Table 2. On the basis of the R^2 value, Langmuir isotherm model had the highest R^2 value compared to Freundlich and Temkin models. Therefore, adsorption of MO dye by modified fly ash-based geopolymer followed Langmuir isotherm model or monolayer adsorption.

In this study, maximum adsorption capacity of MO dye by modified fly ash-based geopolymer was 19.231 mg·g^{-1} with dimensionless separation factor (R_L) of 0.16–0.018 at initial concentration of 10–100 mg·L^{-1} indicating favorable adsorption. The value of R_L can be calculated from the equation:

$$R_L = \frac{1}{1 + K_L C_0} \quad (9)$$

where: K_L – Langmuir constant;
C_0 – initial concentration.

On the basis of the R_L value, adsorption process can be categorized as favorable adsorption ($0<R_L<1$), irreversible adsorption ($R_L=0$), linear adsorption ($R_L=1$), and unfavorable adsorption ($R_L>1$) (Amin et al., 2015; Purbasari et al., 2022). The comparison of obtained result in this research with the others is shown in Table 3. Adsorption of MO dye by modified geopolymer derived from fly ash waste was quite good compared to other adsorbents.

CONCLUSIONS

Modification of fly ash-based geopolymer with CTAB cationic surfactant can increase the adsorption capacity of MO anionic dye on geopolymer. The adsorption of MO dye by modified fly ash-based geopolymer showed the best result at low pH and reached equilibrium after 90 minutes. The adsorption process followed pseudo-second-order kinetics model and Langmuir isotherm model with maximum adsorption capacity of 19.231 mg·g^{-1}.

Acknowledgements

The authors are grateful to DRTPM Ditjen Diktiristek, Kemdikbudristek Republik Indonesia for funding this research through PDUPT 2022.

REFERENCES

1. Al-Ghouti M.A., Al-Absi R.S. 2020. Mechanistic understanding of the adsorption and thermodynamic aspects of cationic methylene blue dye onto cellulosic olive stones biomass from wastewater. Scientific Reports, 10, 15928.
2. Amin M.T., Alazba A.A., Shafiq M. 2015. Adsorptive removal of Reactive Black 5 from wastewater using bentonite clay: Isotherms, kinetics and thermodynamics. Sustainability, 7, 15302–15318.
3. Benjelloun M., Miyah Y., Evrendilek G.A., Zerrouq F., Lairini S. 2021. Recent advances in adsorption kinetic models: Their application to dye types. Arabian Journal of Chemistry, 14(4), 103031.
4. Davidovits J. 2017. Geopolymers: Ceramic-like inorganic polymers. Journal of Ceramic Science and Technology, 8, 335–350.
5. El Alouani M., Alehyen S., El Achouri M., Taibi M. 2019. Comparative studies on removal of textile dye onto geopolymeric adsorbents. EnvironmentAsia, 12(1), 143–153.
6. Fernandes J.V., Rodrigues A.M., Menezes R.R., Neves G.A. 2020. Adsorption of anionic dye on the acid-functionalized bentonite. Materials, 13, 3600.
7. Fumba G., Essomba J.S., Tagne G.M., Nsami J.N., Bélibi P.D.B., Mbadcam J.K. 2014. Equilibrium and kinetic adsorption studies of methyl orange from aqueous solutions using kaolinite, metakaolinite and activated geopolymer as low cost adsorbents. Journal of Academia and Industrial Research, 3(4), 156–163.
8. Huang Z., Li Y., Chen W., Shi J., Zhang N., Wang X., Li Z., Gao L., Zhang Y. 2017. Modified bentonite adsorption of organic pollutants of dye wastewater. Materials Chemistry and Physics, 202, 266–276.
9. Iwuozor K.O, Ighalo J.O., Emenike E.C., Ogunfowora L.A., Igwegbe C.A. 2021. Adsorption of

methyl orange: A review on adsorbent performance. Current Research in Green and Sustainable Chemistry, 4, 100179.

10. Khan M.I., Shanableh A., Elboughdiri N., Lashari M.H., Manzoor S., Shahida S., Farooq N, Bouazzi Y., Rejeb S., Elleuch Z., Kriaa K., Rehman A. 2022. Adsorption of methyl orange from an aqueous solution onto a BPPO-based anion exchange membrane. ACS Omega, 7, 26788–26799.
11. Ma Q., Shen F., Lu X., Bao W., Ma H. 2013. Studies on the adsorption behavior of methyl orange from dye wastewater onto activated clay. Desalination and Water Treatment, 51(19–21), 3700–3709.
12. Mahmoodi N.M., Banijamali M., Noroozi B. 2014. Surface modification and ternary system dye removal ability of manganese ferrite nanoparticle. Fibers and Polymers, 15(8), 1616–1626.
13. Mobarak M., Selim A.Q., Mohamed E.A., Seliem M.K. 2018. A superior adsorbent of CTAB/H_2O_2 solution-modified organic carborich-clay for hexavalent chromium and methyl orange uptake from solutions. Journal of Molecular Liquids, 259, 384–397.
14. Nizam N.U.M., Hanafiah M.M., Mahmoudi E., Halim A.A., Mohammad A.W. 2021. The removal of anionic and cationic dyes from an aqueous solution using biomass-based activated carbon. Scientific Reports, 11, 8623.
15. Purbasari A., Samadhi T.W., Bindar Y. 2018. The effect of alkaline activator types on strength and microstructural properties of geopolymer from co-combustion residuals of bamboo and kaolin. Indonesian Journal of Chemistry, 18(3), 397–402.
16. Purbasari A., Ariyanti D., Sumardiono S., Shofa M.A., Manullang R.P. 2022. Comparison of alkali modified fly ash and alkali activated fly ash as Zn(II) ions adsorbent from aqueous solution. Science of Sintering, 54(1), 49–58.
17. Potgieter J.H., Pardesi C., Pearson S. 2021. A kinetic and thermodynamic investigation into the removal of methyl orange from wastewater utilizing fly ash in different process configurations. Environmental Geochemistry and Health, 43, 2539–2550.
18. Robati D., Mirza B., Rajabi M., Moradi O., Tyagi I., Agarwal S., Gupta V.K. 2016. Removal of hazardous dyes-BR 12 and methyl orange using graphene oxide as an adsorbent from aqueous phase. Chemical Engineering Journal, 284, 687–697.
19. Samadhi T.W., Wulandari W., Prasetyo M.I., Fernando M.R., Purbasari A. 2017. Synthesis of geopolymer from biomass-coal ash blends. AIP Conference Proceedings, 1887, 020031.
20. Selkala T., Suopajarvi T., Sirvio J.A., Luukkonen T., Kinnunen P., de Carvalho A.L.C.B., Liimatainen H. 2020. Surface modification of cured inorganic foams with cationic cellulose nanocrystals and their use as reactive filter media for anionic dye removal. ACS Applied Materials & Interfaces, 12, 27745–27757.
21. Selvi S.S.T., Linet J.M., Sagadevan S. 2018. Influence of CTAB surfactant on structural and optical properties of CuS and CdS nanoparticles by hydrothermal route. Journal of Experimental Nanoscience, 13(1), 130–143.
22. Siyal A.A., Shamsuddin M.R., Khan M.I., Rabat N.E., Zulfiqar M., Man Z., Siame J, Azizli K.A. 2018. A review on geopolymers as emerging materials for the adsorption of heavy metals and dyes. Journal of Environmental Management, 224, 327–339.
23. Wang J., Guo X. 2020. Adsorption isotherm models: Classification, physical meaning, application and solving method. Chemosphere, 258, 127279.
24. Wu L., Liu X., Lv G., Zhu R., Tian L., Liu M., Li Y., Rao W., Liu T., Liao L. 2021. Study on the adsorption properties of methyl orange by natural one-dimensional nano-mineral materials with diferent structures. Scientific Reports, 11, 10640.
25. Xu J., Li M., Zhao D., Zhong G., Sun Y., Hu X., Sun J., Li X., Zhu W., Li M., Zhang Z., Zhang Y., Zhao L., Zheng C., Sun X. 2022. Research and application progress of geopolymers in adsorption: A review. Nanomaterials, 12, 3002.
26. Yu J., Zou A., He W., Liu B. 2020. Adsorption of mixed dye system with cetyltrimethylammonium bromide modified sepiolite: Characterization, performance, kinetics and thermodynamics. Water, 12, 981.